How to Cite: Korolkov, I.V., Ludzik, K., Lisovskaya, L.I., Zibert, A.V., Yeszhanov, A.B., & Zdorovets, M.V. Modification of magnetic Fe_3O_4 nanoparticles for targeted delivery of payloads**.** *Bulletin of the University of Karaganda – Chemistry, 101(1), 99-108.* https://doi.org/10.31489/2021Ch1/99-108

UDC 544.77, 547.1, 546.05 https://doi.org/10.31489/2021Ch1/99-108

I.V. Korolkov[1, 2*], K. Ludzik[3, 4], L.I. Lisovskaya[1], A.V. Zibert[2], A.B. Yeszhanov[1, 2], M.V. Zdorovets[1, 2]

[1]*Institute of Nuclear Physic of the Republic of Kazakhstan, Almaty, Kazakhstan;*
[2]*L.N. Gumilyov Eurasian National University, Nur-Sultan, Kazakhstan;*
[3]*Department of Physical Chemistry, University of Lodz, Poland;*
[4]*Frank Laboratory of Neutron Physics, Joint Institute for Nuclear Research, Dubna, Russia*
*(*Corresponding author's e-mail: i.korolkov@inp.kz)*

Modification of magnetic Fe_3O_4 nanoparticles for targeted delivery of payloads

The development of methods for targeted delivery of payload is a rapidly developing area of research. For this reason, iron oxide nanoparticles have potential to be used in delivery of substances by using external magnetic field. However it is necessary to develop methods of their modification, which will lead to the possibility of immobilization of payloads with the required concentration for therapeutic use. In this article, supermagnetic iron oxide nanoparticles (Fe_3O_4) were modified with silanes such as (3-chloropropyl)-trimethoxysilane, (3-mercaptopropyl)trimethoxysilane, (3-aminopropyl)trimethoxysilane and (3-glycidyl-propyl)trimethoxysilane by reaction of polycondensation. Then carborane compound (payload) was successfully attached on the modified nanoparticles via covalent bonding. Structure, size and element composition were studied by Fourier-transform infrared spectroscopy (FTIR), scanning electron microscopy (SEM) and Energy-dispersive X-ray spectroscopy (EDA). It was found that resulting nanoparticles contain 16.6 % of boron (according to EDA), and their average size is 32±9 nm (according to SEM). In vitro test using HeLa (cervical cancer cell) and PC-3 (prostate cancer cell) shows low cytotoxicity in concentration range of 1–200 μg/ml.

Keywords: Fe_3O_4 nanoparticles, silane, surface modification, targeted delivery of payload, BNCT, carborane, biological test, cytotoxicity.

Introduction

The science and engineering of nanometer-sized materials is currently being used to develop numerous scientific, industrial, environmental, and technological fields. Biology, medicine, chemistry, pharmaceuticals, agriculture, food industry and materials science are the main areas that have benefited from the technological progress achieved in the field of nanoscience. In recent years, significant growth has been observed in the biomedical application of nanostructured materials [1–4]. Nanostructures of different composition and shapes form the basis for a huge variety of pharmaceutical and medical applications, including diagnosis and drug delivery, and they have particular potential in cancer therapy. According to the International Agency for Research on Cancer [5], 18.1 million new cancer cases and 9.6 million cancer deaths were reported in 2018. Kazakhstan mortality index is 140.2 while average of worldwide is 102.4 and it is predicted that this index will grow. Despite all the preventive measures and therapeutic efforts of the last decades, the upward trend in incidence continues [6]. Typical chemotherapy drugs cannot be sufficiently concentrated in the area of the tumor and have a negative effect on the entire body. Thus, one of the problems is the development of methods of targeted therapy, which selectively affects the tumor, while maintaining healthy tissue and increasing the effectiveness of the drugs used. Biomimetic properties as well as an unusual surface-to-volume ratio make nanoparticles promising tools for the treatment of diseases [1].

Nanoparticles have unique physical and chemical properties due to their size, which can be comparable with the sizes of antibodies, receptors, nucleic acids, proteins, and other biological macromolecules. In addition, the use of nanostructures may allow the use of compounds that have poor solubility in water or low chemical and biological stability, metabolic barriers and etc. For these purposes, various nanostructures are used: liposomes, polymer and protein nanocapsules, micelles, gold and silicon nanoparticles [7]. Moreover, magnetic iron oxide nanoparticles have wide potential applications in biomedicine [8–12], including magnetic resonance imaging, magnetic hyperthermia, cancer therapy, and targeted drug delivery; in catalysis [13–15] and magnetic separation [16, 17]. Despite these promising results, their successful transition into clinical conditions depends strongly on their physicochemical properties, toxicity, and functionalization possibilities. Iron oxide nanoparticles are low stable, have a tendency to agglomerate in solutions, they have lack of bio-

compatibility. Various materials, such as silanes, metals, polymers, fatty acids and amino acids, are used to functionalize the surface and to stabilize magnetic nanoparticles [18–20]. Among other materials, silane based compounds are the most promising because they have high biocompatibility, stability, low toxicity, low cost, and high capacity for functionalization [21–23]. Moreover, the modification of magnetic nanoparticles with silanes with various functional groups will allow immobilization of drugs with different chemical nature. One of such drugs can be carborane derivatives for potential use in neutron capture cancer therapy (NCT) and chemotherapeutic drugs.

In this article, we present the results of synthesis and modification of iron oxide nanoparticles with various silanes and immobilization of carborane compound (payload) on their surface. Moreover, the biocompatibility was evaluated in vitro using human cancer cell lines: HeLa (cervical cancer cell) and PC-3 (prostate cancer cell).

Experimental

Synthesis and modification of iron oxide nanoparticles

Fe_3O_4 nanoparticles were obtained by co-precipitation of a mixture of iron chloride (II) and iron chloride (III) with the addition of ammonium hydroxide according to the method described in the our previous published article [24].

Modification of the surface of iron oxide nanoparticles with silanes such as (3-chloropropyl)-trimethoxysilane (Si-Cl), (3-mercaptopropyl)trimethoxysilane (Si-SH), (3-aminopropyl)trimethoxysilane (Si-NH_2) and (3-glycidylpropyl)trimethoxysilane (Si-epoxy) was performed by reaction of polycondensation. With this aim, 0.5 g of Fe_3O_4 was dispersed in 100 ml of o-xylene, 3 ml of silane was added, the reaction mixture was purged with argon. The reaction was carried out at 90 ºC for 5 hours. After that, the obtained nanoparticles were separated with a magnet, washed in o-xylene, acetone, and dried.

Immobilization of carboranes to functionalized Fe_3O_4 nanoparticles

Commercial available isopropyl-o-carborane (0.016 M) was dissolved in 30 ml anhydrous benzene. The solution was bubbled with argon, then freshly prepared butyl lithium solution (0.016 M) was added, isopropyl-o-carboranyl lithium was precipitated after 1 hour of stirring. Diethyl ether was added to the reaction mixture to dissolve the precipitate. After that, suspension of Fe_3O_4–Si-epoxy in benzene was added. The reaction was carried out at room temperature during 6 hours. The resulting suspension was magnetically separated, washed with benzene and diethyl ether several times, dried at 50 ºC.

Methods of characterization

FTIR spectra were recorded on InfraLum FT-08 FTIR Spectrometer (Lumex, Russia) with Single Reflection Diamond ATR accessory (GladiATR, PIKE) to study chemical group shifts before and after nanoparticles modification. Measurements were taken in the range of 400 to 4000 cm^{-1}. All spectra (25 scans at 2 cm^{-1} resolution) were recorded at 21–25 ºC.

JEOL JSM-7500F scanning electron microscope (SEM) was used for characterization of nanoparticle morphology and size during functionalization. Nanoparticle distribution were evaluated by analyzing SEM images using ImageJ. EDX analysis was done using Hitachi TM 3030 with microanalysis system Bruker XFlash MIN SVE at 15 kV. Before the analysis, the samples were glued to carbon tape and sputtered with gold on magnetron JFC-1600. The analysis of the elemental composition was carried out evaluating the spectra from various points of the sample, the average values of the element content were calculated based on the 10 spectra.

Cytotoxicity Assay

In order to monitor the cytotoxic effect of functionalised magnetic nanoparticles different human cancer cell lines were used: HeLa (cervical cancer cell), PC-3 (prostate cancer cell). As recommended, fibroblasts like cells of L929 obtained from subcutaneous adipose tissue of mouse were used as normal cells (PN-EN ISO 10993–5:2009 norm). The cell culture for HeLa and PC-3 was described previously [25].

Cytotoxicity of nanoparticles was evaluated using in vitro model and day 3-(4,5-dimethylthiazol-2-yl)-2,5-diphenyltetrazolium bromide [26, 27]. All cancer cell lines were plated into 96-well plates in volume of $8–10 \cdot 10^3$/100 µl/well. After 24 hours incubation, the samples were added in a concentration range of 1–200 µg/ml and a volume of 100 µl/well into wells with suspensions of particular cell lines. Subsequently, cells were incubated for next 24 hours and 72 hours under standard conditions (37 ºC and 5 % CO_2). In experiments two types of cell culture medium were used: with fetal bovine serum (FBS+) and without (FBS–). After that time, fresh prepared MTT solution (5 mg/1 ml PBS) was added in volume of 20 µl to each well

and cells were incubated for the next 3 hours under the same conditions. Then, the wells contents were removed and lasting crystals were dissolved by the addition of 100 µl DMSO to each well. Absorbance was measured using BioTek Power Wave XS spectrophotometer at the wavelength of λ=570 nm. Prior to investigation the nanoparticles solution in PBS probes were sonicated in order to disintegrate particles with ultrasounds. Control values were absorbance measurements received for the wells with cells incubated without the addition of the studied compounds. For each concentration of the nanoparticles 6 absorbance measurements were carried out, for which average values ± SEM were calculated. Obtained MTT results were processed using GraphPad Prism 7 Program, into graphs, which depict inhibition of cell viability in relation to compound concentration.

Results and Discussion

At the first stage of the study, methods of coating magnetic iron oxide nanoparticles with a silane shell were studied. Silanes can serve as an intermediate link between inorganic nanoparticles and organic/organoelement payloads. Trimethoxysilanes with different reactive groups such as chlorine-, amino-, epoxy- and mercapto- were chosen to be able to attach different payloads at next stage. To create the shell, the polycondensation reaction of silanes was used, which occurs both with silane molecules and with hydroxyl groups that are on the surface of iron oxide nanoparticles. Thus (3-chloropropyl)trimethoxysilane, (3-mercaptopropyl)trimethoxysilane, (3-aminopropyl)trimethoxysilane and (3-glycidylpropyl)trimethoxysilane were chosen. The reaction was carried out in *o*-xylene under argon. Magnetic separation made it possible to well purify magnetically modified nanoparticles from non-magnetic silane nanoparticles, which were a by-product. Figure 1 shows the results of Fe_3O_4 modification with (3-chloropropyl) trimethoxysilane. It was found out that size of nanoparticles increased from 21±4 nm (initial Fe_3O_4) to 29±5 nm according to SEM analysis. At the same time, the weight gain was 2.8 %. Elemental composition according to EDA analysis is as follows (Fig. 1*c*): Fe — 13 %, O — 43.6 %, C — 40.2 %, Cl — 0.6 %, Si — 0.5 %, Au — 1.1 %, Cu — 1 %. It should be noted that gold and copper appeared as a result of magnetron sputtering before SEM analysis to avoid surface charge. The FTIR spectrum (Fig. 1*d*) of the initial Fe_3O_4 nanoparticles is characterized by absorption at 3500–3000 cm^{-1} (OH), 1614 cm^{-1} associated with O–H vibrations in combination with Fe atoms, as well as at 544 and 399 cm^{-1} (Fe–O). The coating of nanoparticles led to the appearance of new peaks at 1040 and 1146 cm^{-1} (Si–O–Si) and 628 cm^{-1} (C–Cl). The absence of peak at 913 and 940 cm^{-1} allow us to conclude that the reaction of polycondensation completed.

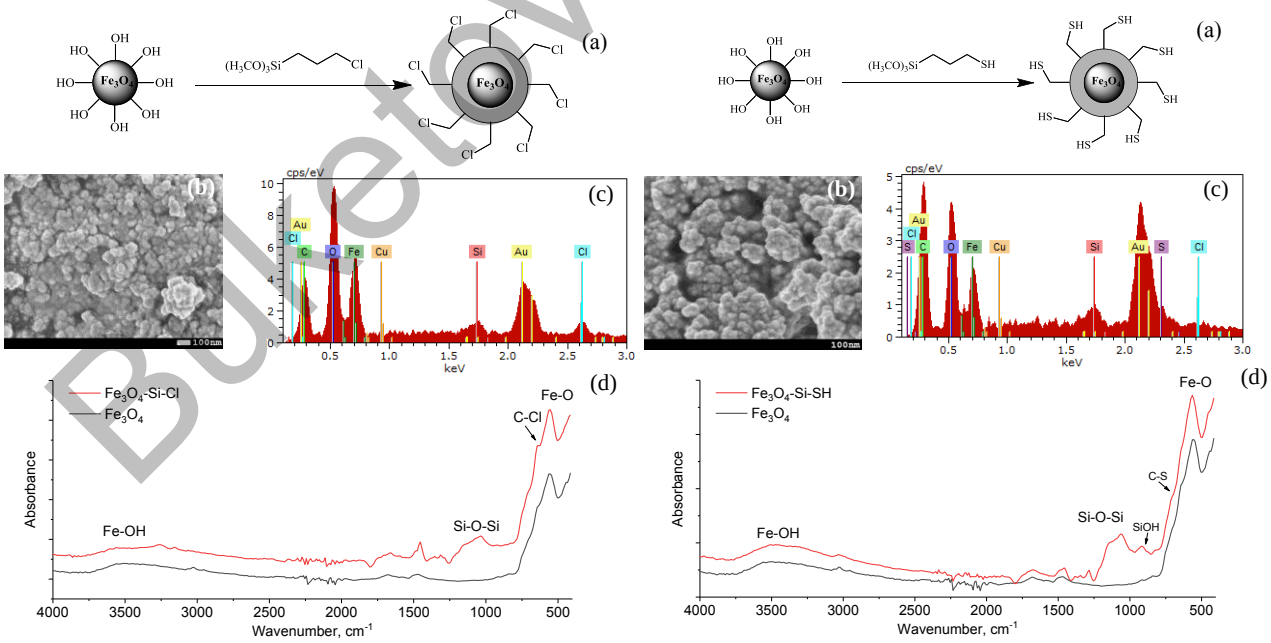

Figure 1. Scheme of modification of Fe_3O_4 by (3-chloropropyl)trimethoxysilane (*a*), SEM image (*b*), EDA (*c*) and FTIR spectra (*d*)

Figure 2. Scheme of modification of Fe_3O_4 by (3-mercaptopropyl)trimethoxysilane (*a*), SEM image (*b*), EDA (*c*) and FTIR spectra (*d*)

Modification with (3-mercaptopropyl)-trimethoxysilane led to formation of nanoparticles with size of 26±6 nm (Fig. 2*b*). The FTIR spectra (Fig. 2*d*) show the appearance of new peaks at 706 cm^{-1} (S–C), 1059 and 1144 cm^{-1} (Si–O–Si). At the time the broad peak at 913 cm^{-1} were detected which is related to Si–OH group. This indicates the incompleteness of the reaction. EDA (Fig. 2*c*) registered 1.3 % of sulfur and 1.5 % of silicon.

Modification with (3-aminopropyl) trimethoxysilane was carried out according to the same procedure in o-xylene at 90 ºC. The average size of obtained nanoparticles was 30±8 nm. Aminated nanoparticles are characterized by the appearance of new peaks at 1677 cm^{-1} (NH_2), at 1163 and 1064 cm^{-1} (Si–O–Si), and at 1265 cm^{-1} (C–N) (Fig. 3). It was also found out appearance the peak related to Si–OH bonds, but with a lower concentration than in the case of (3-mercaptopropyl)trimethoxysilane. Nitrogen in the amount of 7.6 % was observed in EDA. Modification of Fe_3O_4 by (3-glycidylpropyl)trimethoxysilane allowed to create chemical active epoxy groups for further isopropyl-o-carborane attachment (payload). Epoxy ring were detected in FTIR spectra at around 900–920 cm^{-1}. In the same region, the peak related to Si–OH can be appeared. The presence of the epoxy group will also be confirmed by further chemical transformations. SEM analysis (Fig. 4*b*) shows an average nanoparticles size of 39±8 nm.

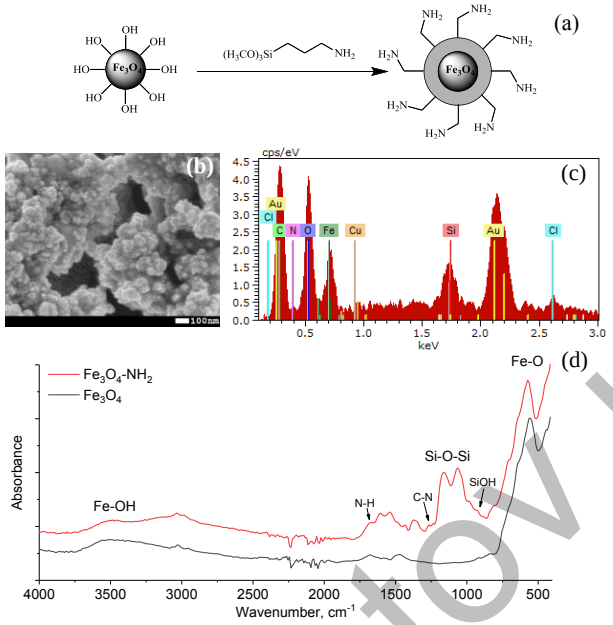

Figure 3. Scheme of modification of Fe_3O_4 by (3-aminopropyl)trimethoxysilane (*a*), SEM image (*b*), EDA (*c*) and FTIR spectra (*d*)

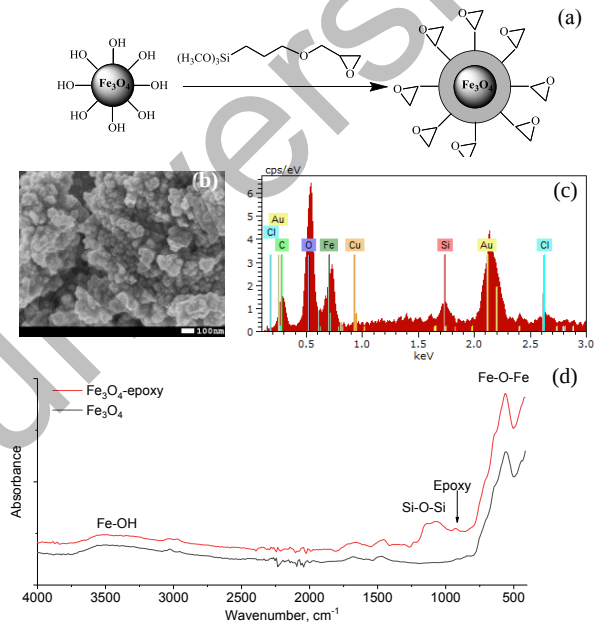

Figure 4. Scheme of modification of Fe_3O_4 by (3-glycidylpropyl)trimethoxysilane (*a*), SEM image (*b*), EDA (*c*) and FTIR spectra (*d*)

Commercial available isopropyl-*o*-carborane was immobilized to Fe_3O_4-Si-epoxy nanoparticles via covalent bonding using butyl lithium as shown in Figure 5*a*. New peaks in FTIR spectra (Fig. 5*d*) appeared at 3353, 2924, 2572, 1496, 1433 and 860 cm^{-1} are related to OH, C–H, B–H, δ_{as} CH_3 and carborane skeleton vibrations respectively [29], with increase in average nanoparticles size according to SEM analysis to 32 ± 9 nm (Fig. 5b-c).

EDA analysis was performed to study element content on Fe_3O_4 nanoparticles surface before and after modification. The data extracted from the EDA spectra are collected in Table 1. Initial Fe_3O_4 consist of 43.1 % Fe and 56.9 % O. Isopropyl-*o*-carborane attachment led to the appearance of boron in an amount of 16.5 %.

Table 1

Data from EDA spectra

Sample	Atomic content, %				
	Fe	O	Si	B	C
Initial Fe_3O_4	43.1±2.1	56.9±3.6	–	–	–
Fe_3O_4/GPTMS	20.7±2.1	52.9±2.1	6.4±1.3	–	20.0±1.5
Fe_3O_4/GPTMS/Carborane	22.2±1.5	38.9±3.1	2.4±0.3	16.5±2.3	20.0±1.4

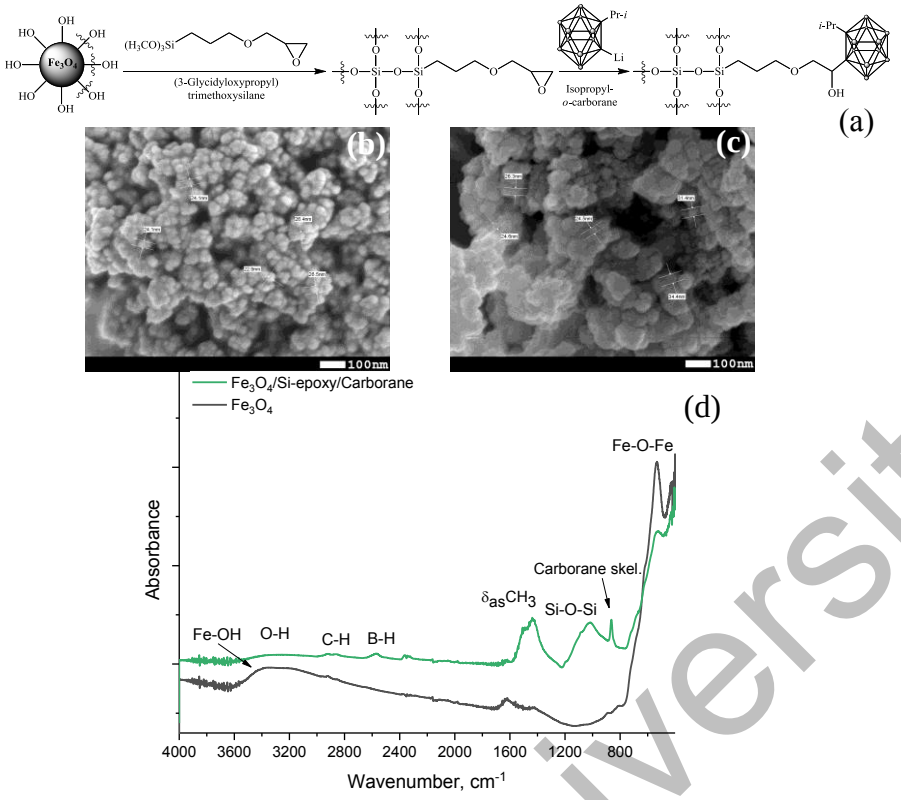

Figure 5. Scheme of Fe_3O_4 modification and carborane immobilization (*a*), SEM image of initial Fe_3O_4 nanoparticles (*b*), SEM image of Fe_3O_4-Si-epoxy-carborane nanoparticles (c) and FTIR spectra of Fe_3O_4 before and after modification (*d*)

Results of XRD analysis of the studied nanoparticles before and after modification are presented in Figure 6. The general view of X-ray diffraction patterns evidence to the polycrystalline type of nanoparticles with a low degree of structural ordering and crystallinity. Table 2 shows the results of changes in structural parameters calculated based on the analysis of X-ray diffraction patterns, which were made according to [30–31].

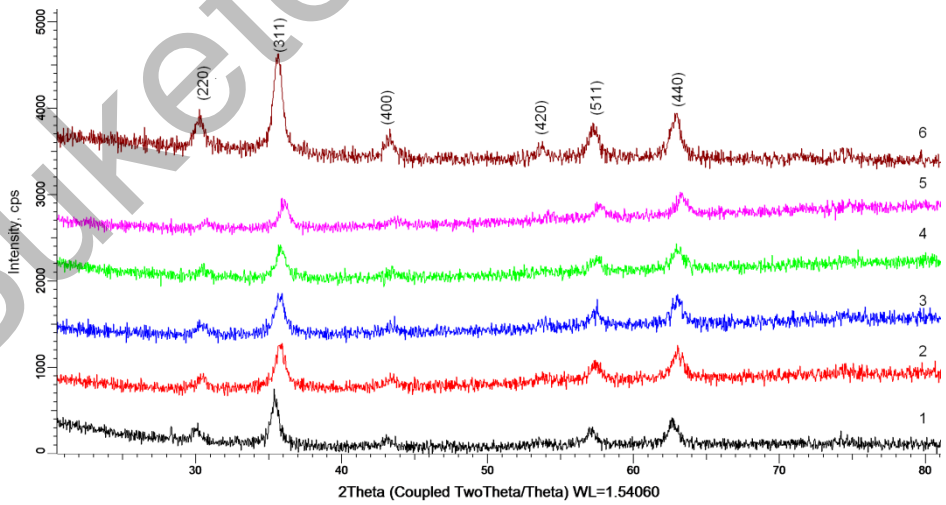

1 — initial Fe_3O_4; *2* — Fe_3O_4-Si-Cl; *3* — Fe_3O_4-Si-SH; *4* — Fe_3O_4-Si-epoxy; *5* — Fe_3O_4-Si-epoxy-carboranes; *6* — Fe_3O_4-Si-NH_2

Figure 6. XRD patterns

Table 2

Data of XRD analysis

Sample	Initial Fe_3O_4	Fe_3O_4-Si-Cl	Fe_3O_4-Si-SH	Fe_3O_4-Si-NH_2	Fe_3O_4-Si-epoxy	Fe_3O_4-Si-epoxy-carboranes
Structure type	Cubic Fd-3m(227) PDF-00–065–0731					
Lattice parameter, Å	a = 8.4226	a = 8.3384	a = 8.3139	a = 8.3429	a = 8.3039	a = 8.2603
δ	0.009	0.02	0.193	0.091	0.206	0.234
Structure	$Fe_{2.99}O_4$	$Fe_{2.98}O_4$	$Fe_{2.81}O_4$	$Fe_{2.91}O_4$	$Fe_{2.80}O_4$	$Fe_{2.77}O_4$
Crystalline size, nm	18.92±1.86	14.89±1.54	21.33±1.78	18.03±1.69	17.82±1.49	17.41±1.39

It was found that with a high degree of probability (more than 85 %), the diffraction pattern of the obtained nanoparticles corresponds to the cubic phase of magnetite, with the spatial system Fd-3m (227). Comparison analysis was carried out using the PDF-2 database. In this case, the parameters of the crystal lattice differ from the reference values selected from the PDF-00-065-0731 database. The differences can be caused both by the processes of disordering of the structure arising as a result of synthesis, as well as by subsequent oxidation processes associated with the processes of modification. In this case, the modification leads both to a change in the stoichiometric ratio and in the crystallite size.

The cytotoxicity of Fe_3O_4-Si-epoxy-Carborane nanoparticles was characterized by determination of cell vitality. The percentages of active cells — cell viability ± SEM values after 24h and 72 hours incubation are shown in Figure 7.

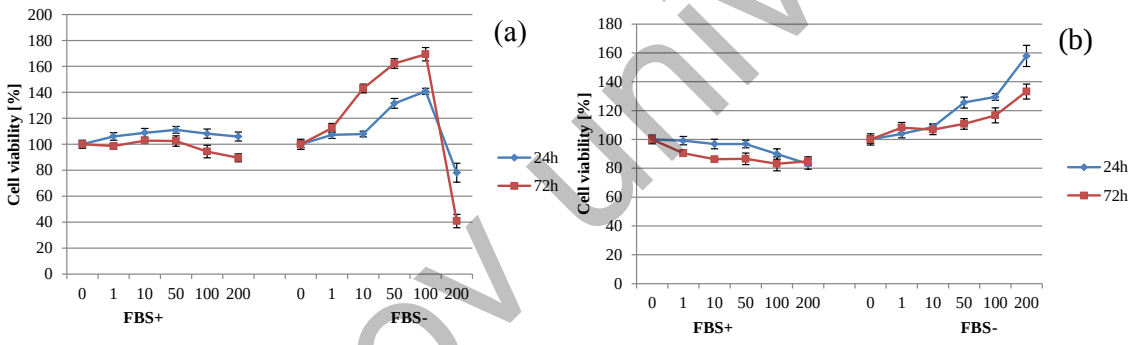

Figure 7. Cell viability after 24 and 72 hours incubation with FBS and without FBS as a function of nanoparticles concentrations for HeLa (*a*) and PC-3 (*b*) cell lines

Visual inspection of cells along with the viability and cytotoxicity after 24 hours as well as 72 hours incubation results indicated a low cytotoxicity of investigated particles for concentrations < 200μg/ml in case all investigated cell lines. For that reason, the value of IC50 (half maximal inhibitory concentration) has not been established. The dose-dependent decrease in viability is well visible for HeLa and PC-3 cells. The experiments indicate that mitochondrial and overall cell viability is maintained. Unexpected increase in viability visible especially for medium without (FBS-) may be due to increased mitochondrial activity associated with cell phagocytosis of nanoparticles.

Conclusions

Functionalization of Fe_3O_4 nanoparticles with epoxy, amino, mercapto, chloro group using silanes was carried out. The features of the reactions were studied; the optimal conditions for the process were established. The formation of functional groups has been proven by FTIR spectroscopy, SEM, and EDA. Further, the obtained modified nanoparticles with chemically active groups can be used to immobilize payload. For this propose, carborane compound was successfully attached to the modified nanoparticles via formation of covalent bond for potential application in boron neutron capture therapy of cancer. It was found that resulting nanoparticles contain 16.6 % of boron (according to EDA), and their average size is 32±9 nm (according to SEM). In vitro test using HeLa (cervical cancer cell) and PC-3 (prostate cancer cell) shows low cytotoxicity in concentration range of 1–200 μg/ml.

This study was funded by the Ministry of Education and Science of the Republic of Kazakhstan (grant No AP08051954) and Joint Institute for Nuclear Research-Republic of Kazakhstan cooperation program (Order No. 391, 20.07.2020).

References

1 Anselmo A.C. Nanoparticles in the clinic / A.C. Anselmo, S. Mitragotri // Bioeng. Transl. Med. — 2016. — Vol. 1, No. 1. — P. 10–29. https://doi.org/10.1002/btm2.10003

2 Cruz M.M. Nanoparticles for magnetic hyperthermia / M.M. Cruz, L.P. Ferreira, A.F. Alves, S.G. Mendo, P. Ferreira, M. Godinho, M.D. Carvalho // Nanostructures Cancer Ther. — 2017. — P. 485–511. https://doi.org/10.1016/B978-0-323-46144-3.00019-2

3 Meola A. Magnetic Particle Imaging in Neurosurgery / A. Meola, J. Rao, N. Chaudhary, G. Song, X. Zheng, S.D. Chang // World Neurosurg. — 2019. — Vol. 125. — P. 261–270. https://doi.org/10.1016/j.wneu.2019.01.180

4 Doswald S. Biochemical functionality of magnetic particles as nanosensors: how far away are we to implement them into clinical practice? / S. Doswald, W.J. Stark, B. Beck-Schimmer // J. Nanobiotechnology. — 2019. — Vol. 17, No.1. — P. 1–11. https://doi.org/10.1186/s12951–019–0506-y

5 Bray F. Global cancer statistics 2018: GLOBOCAN estimates of incidence and mortality worldwide for 36 cancers in 185 countries / F. Bray, J. Ferlay, I. Soerjomataram, R.L. Siegel, L.A. Torre, A. Jemal // CA. Cancer J. Clin. — 2018. — Vol. 68. — P. 394–424. https://doi.org/10.3322/caac.21492

6 Tietze R. Magnetic nanoparticle-based drug delivery for cancer therapy / R. Tietze, J. Zaloga, H. Unterweger, S. Lyer, R.P. Friedrich, C. Janko, M. Pöttler, S. Dürr // Biochem. Biophys. Res. Commun. — 2015. — Vol. 468. — P. 463–470. https://doi.org/10.1016/J.BBRC.2015.08.022

7 Wolfram J. Clinical cancer nanomedicine / J. Wolfram, M. Ferrari // Nano Today. — 2019. — Vol. 25. — P. 85–98. https://doi.org/10.1016/j.nantod.2019.02.005

8 Remya N. Toxicity, toxicokinetics and biodistribution of dextran stabilized Iron oxide Nanoparticles for biomedical applications / N.S. Remya, S. Syama, A. Sabareeswaran, P.V. Mohanan // Int. J. Pharm. — 2016. — Vol. 511. — P. 586–598. https://doi.org/10.1016/J.IJPHARM.2016.06.119

9 Chandra S. PEGylated Iron Oxide Nanoparticles for pH Responsive Drug Delivery Application / S. Chandra Mohanta, A. Saha, P. Sujatha Devi // Mater. Today Proc. — 2018. — Vol. 5. — P. 9715–9125.

10 Hauser A.K. Targeted iron oxide nanoparticles for the enhancement of radiation therapy / A.K. Hauser, M.I. Mitov, E.F. Daley, R.C. McGarry, K.W. Anderson, J.Z. Hilt // Biomaterials. — 2016. — Vol. 105. — P. 127–135. https://doi.org/10.1016/J.BIOMATERIALS.2016.07.032

11 Shelat R. Detailed toxicity evaluation of β-cyclodextrin coated iron oxide nanoparticles for biomedical applications / R. Shelat, S. Chandra, A. Khanna // Int. J. Biol. Macromol. — 2018. — Vol. 110. — P. 357–365. https://doi.org/10.1016/J.IJBIOMAC.2017.09.067

12 Dadfar S.M. Iron oxide nanoparticles: Diagnostic, therapeutic and theranostic applications / S.M. Dadfar, K. Roemhild, N.I. Drude, S. von Stillfried, R. Knüchel, F. Kiessling, T. Lammers // Adv. Drug Deliv. Rev. — 2019. — Vol. 138. — P. 302–325. https://doi.org/10.1016/J.ADDR.2019.01.005

13 Rajabi F. Oxidative esterification of alcohols and aldehydes using supported iron oxide nanoparticle catalysts / F. Rajabi, R.A.D. Arancon, R. Luque // Catal. Commun. — 2015. — Vol. 59. — P. 101–103. https://doi.org/10.1016/J.CATCOM.2014.09.022

14 Pizzolato E. Water oxidation electrocatalysis with iron oxide nanoparticles prepared via laser ablation / E. Pizzolato, S. Scaramuzza, F. Carraro, A. Sartori, S. Agnoli, V. Amendola, M. Bonchio, A. Sartorel // J. Energy Chem. — 2016. — Vol. 25. — P. 246–250. https://doi.org/10.1016/J.JECHEM.2015.12.004

15 Devi H.S. Singh, Iron oxide nanoparticles synthesis through a benign approach and its catalytic application / H.S. Devi, T.D. Singh // Perspect. Sci. — 2016. — Vol. 8. — P. 287–289.

16 Nebu J. Fluorescence turn-on detection of fenitrothion using gold nanoparticle quenched fluorescein and its separation using superparamagnetic iron oxide nanoparticle / J. Nebu, J.S. Anjali Devi, R.S. Aparna, B. Aswathy, G.M. Lekha, G. Sony // Actuators B Chem. — 2018. — Vol. 277. — P. 271–280. https://doi.org/10.1016/J.SNB.2018.08.153

17 van de Loosdrecht M.M. Separation of excitation and detection coils for in vivo detection of superparamagnetic iron oxide nanoparticles / M.M. van de Loosdrecht, S. Waanders, H.J.G. Krooshoop, B. ten Haken // J. Magn. Magn. Mater. — 2019. — Vol. 475. — P. 563–569. https://doi.org/10.1016/J.JMMM.2018.12.012

18 Ozel F. Characterization of tartaric acid and ascorbic acid coated iron oxide nanoparticles and their biocompatibility studies / F. Ozel, E. Tokay, F. Köçkar, H. Köçkar // J. Magn. Magn. Mater. — 2018. — Vol. 474. — P. 654–660. https://doi.org/10.1016/J.JMMM.2018.11.025

19 Yathindranath V. Thliveris, One-Pot Synthesis of Iron Oxide Nanoparticles with Functional Silane Shells: A Versatile General Precursor for Conjugations and Biomedical Applications / V. Yathindranath, Z. Sun, M. Worden, L.J. Donald, J.A., J.A. Thliveris // Langmuir. — 2013. — Vol. 29. — P. 10850–10858.

20 Özgür M. The Toxicity Assessment of Iron Oxide (Fe_3O_4) Nanoparticles on Physical and Biochemical Quality of Rainbow Trout Spermatozoon / M. Özgür, A. Ulu, S. Balcıoğlu, İ. Özcan, S. Köytepe, B. Ateş // Toxics. — 2018. — Vol. 6. — P. 62. https://doi.org/10.3390/toxics6040062

21 Fernández-Bertólez N. Toxicological assessment of silica-coated iron oxide nanoparticles in human astrocytes / N. Fernández-Bertólez, C. Costa, F. Brandão, G. Kiliç, J.A. Duarte, J.P. Teixeira, E. Pásaro, V. Valdiglesias, B. Laffon // Food Chem. Toxicol. — 2018. — Vol. 118. — P. 13–23. https://doi.org/10.1016/J.FCT.2018.04.058

22 Janko C. Strategies to optimize the biocompatibility of iron oxide nanoparticles — «SPIONs safe by design / C. Janko, J. Zaloga, M. Pöttler, S. Dürr, D. Eberbeck, R. Tietze, S. Lyer, C. Alexiou // J. Magn. Magn. Mater. — 2017. — Vol. 431. — P. 281–284. https://doi.org/10.1016/J.JMMM.2016.09.034

23 Kurczewska J. Preparation of multifunctional cascade iron oxide nanoparticles for drug delivery / J. Kurczewska, M. Cegłowski, G. Schroeder // Mater. Chem. Phys. — 2018. — Vol. 211. — P. 34–41. https://doi.org/10.1016/J.MATCHEMPHYS.2018.01.064

24 Tishkevich D.I. Immobilization of boron-rich compound on Fe_3O_4 nanoparticles: Stability and cytotoxicity / D.I. Tishkevich, I.V. Korolkov, A.L. Kozlovskiy, M. Anisovich, D.A. Vinnik, A.E. Ermekova, A.I. Vorobjova, E.E. Shumskaya, T.I. Zubar, S.V. Trukhanov, M.V. Zdorovets // J. Alloys Compd. — 2019. — Vol. 794. — P. 573–581. https://doi.org/10.1016/j.jallcom.2019.05.075

25 Kozlovskiy A.L. Study of phase transformations, structural, corrosion properties and cytotoxicity of magnetite-based nanoparticles / A.L. Kozlovskiy, A.E. Ermekova, I.V. Korolkov, D. Chudoba, M. Jazdzewska, K. Ludzik, A. Nazarova, B. Marciniak, R. Kontek, A.E. Shumskaya, M.V. Zdorovets // Vacuum. — 2019. — Vol. 163. — P. 236–247. https://doi.org/10.1016/J.VACUUM.2019.02.029

26 Stockert J.C. Tetrazolium salts and formazan products in Cell Biology: Viability assessment, fluorescence imaging, and labeling perspectives / J.C. Stockert, R.W. Horobin, L.L. Colombo, A. Blázquez-Castro // Acta Histochem. — 2018. — Vol. 120. — P. 159–167. https://doi.org/10.1016/j.acthis.2018.02.005

27 Abe K. Measurement of cellular 3-(4,5-dimethylthiazol-2-yl)-2,5-diphenyltetrazolium bromide (MTT) reduction activity and lactate dehydrogenase release using MTT / K. Abe, N. Matsuki // Neurosci. Res. — 2000. — Vol. 38. — P. 325–329. https://doi.org/10.1016/S0168-0102(00)00188-7

28 Rubio F. A FT-IR study of the hydrolysis of Tetraethylorthoselicate (TEOS) / F. Rubio, J. Rubio, J.L. Oteo // Spectrosc. Lett. — 1998. — Vol. 31. — P. 199–219. https://doi.org/10.1080/00387019808006772

29 Leites L.A. Vibrational Spectroscopy of Carboranes and Parent Boranes and Its Capabilities in Carborane Chemistry / L.A. Leites // Chem. Rev. — 1992. — Vol. 92. — P. 279–323.

30 Bondarenko L.S. Effects of Modified Magnetite Nanoparticles on Bacterial Cells and Enzyme Reactions/ L.S. Bondarenko, E.S. Kovel, K.A. Kydralieva, G.I. Dzhardimalieva, E. Illés, E. Tombácz, A.G. Kicheeva, N.S. Kudryasheva // Polymers. — 2020. — Vol. 10. — P. 1499. https://doi.org/10.3390/nano10081499

31 Bondarenko L.S. Effects of Humic Acids on the Ecotoxicity of Fe_3O_4 Nanoparticles and Fe-Ions: Impact of Oxidation and Aging/ L.S. Bondarenko, A. Kahru, V. Terekhova, G. Dzhardimalieva, P. Uchanov, K. Kydralieva // Nanomaterials. — 2020. — Vol. 10. — P. 1–18. https://doi.org/10.3390/nano10102011

И.В. Корольков, К. Луджик, Л.И. Лисовская,
А.В. Зиберт, А.Б. Есжанов, М.В. Здоровец

Пайдалы жүктемені жеткізу үшін магнитті Fe_3O_4 нанобөлшектерін модификациялау

Пайдалы жүктемені мақсатты жеткізу әдістерін жасау — бұл жедел дамып келе жатқан зерттеу бағыты. Осыған байланысты темір оксидінің нанобөлшектері сыртқы магнит өрісін пайдаланып заттарды жеткізу үшін пайдаланылуы мүмкін. Алайда терапиялық қолдану үшін қажетті концентрациядағы дәрілік заттарды иммобилизациялау мүмкіндігіне әкелетін оларды модификациялау әдістерін әзірлеу қажет. Мақалада (3-хлоропропил)триметоксисилан, (3-меркаптопропил)триметоксисилан, (3-аминопропил)триметоксисилан және (3-глидицилпропил)триметоксисилан сияқты силандармен супермагниттік (Fe_3O_4) темір оксиді нанобөлшектері модификацияланды. Содан кейін карборанды қосылыс модификацияланған нанобөлшектерде коваленттi байланыс түзу арқылы сәтті иммобилизденді. Құрылымы, мөлшері және элементтік құрамы ИҚ-Фурье трансформациялық инфрақызыл спектроскопиясы (ИҚ), сканерлейтін электронды микроскопия (СЭМ) және энергодисперсиялық рентген спектроскопиясы (ЭДС) көмегімен зерттелді. Алынған нанобөлшектерде (ЭДС деректері бойынша) 16,6 % бор бар екендігі анықталды, ал олардың орташа мөлшері (СЭМ деректері бойынша) 34±9 нм. *In vitro* тест HeLa (жатыр мойны обыры жасушалары) және PC-3 (қуық асты безінің қатерлі ісігі жасушалары) үшін 1–200 мкг/мл концентрация ауқымында төмен цитотоксикалықты көрсетеді.

Кілт сөздер: Fe_3O_4 нанобөлшектері, силан, беттік модификациялау, пайдалы жүктемені мақсатты жеткізу, БНҰТ, карборан, биологиялық сынақ, цитотоксикалық.

И.В. Корольков, К. Луджик, Л.И. Лисовская,
А.В. Зиберт, А.Б. Есжанов, М.В. Здоровец

Модификация магнитных наночастиц Fe_3O_4 для адресной доставки полезного груза

Разработка методов адресной доставки полезного груза — быстро развивающееся направление исследований. В связи с этим наночастицы оксида железа потенциально могут быть использованы для доставки веществ с помощью внешнего магнитного поля. Однако необходимо разработать методы их модификации, которые приведут к возможности иммобилизации лекарственных веществ необходимой концентрации для терапевтического использования. В статье супермагнитные наночастицы оксида железа (Fe_3O_4) были модифицированы силанами, такими как (3-хлорпропил)триметоксисилан, (3-меркаптопропил)триметоксисилан, (3-аминопропил)триметоксисилан и (3-глицидилпропил)триметоксисилан. Затем карборановое соединение было успешно иммобилизовано на модифицированные наночастицы посредством образования ковалентной связи. Структура, размер и элементный состав изучены с помощью инфракрасной спектроскопии с преобразованием Фурье (ИК), сканирующей электронной микроскопии (СЭМ) и энергодисперсионной рентгеновской спектроскопии (ЭДА). Было обнаружено, что полученные наночастицы содержат 16,6 % бора (по данным ЭДА), а их средний размер составляет 34±9 нм (по данным СЭМ). Тест *in vitro* показывает низкую цитотоксичность в диапазоне концентраций 1–200 мкг/мл для HeLa (клетки рака шейки матки) и PC-3 (клетки рака простаты).

Ключевые слова: наночастицы Fe_3O_4, силан, модификация поверхности, адресная доставка полезного груза, БНЗТ, карборан, биологический тест, цитотоксичность.

References

1 Anselmo, A.C., & Mitragotri, S. (2016). Nanoparticles in the clinic. *Bioeng. Transl. Med., 1(1),* 10–29. https://doi.org/10.1002/btm2.10003

2 Cruz, M.M., Ferreira, L.P., Alves, A.F., Mendo, S.G., Ferreira, P., & M. Godinho et al. (2017). Nanoparticles for magnetic hyperthermia. *Nanostructures Cancer Ther., 2017,* 485–511. https://doi.org/10.1016/B978-0-323-46144-3.00019-2

3 Meola, A., Rao, J., Chaudhary, N., Song, G., Zheng, X., & Chang, S.D. (2019). Magnetic Particle Imaging in Neurosurgery. *World Neurosurg, 125*, 261–270. https://doi.org/10.1016/j.wneu.2019.01.180

4 Doswald, S., Stark, W.J., & Beck-Schimmer, B. (2019). Biochemical functionality of magnetic particles as nanosensors: how far away are we to implement them into clinical practice? *J. Nanobiotechnology, 17,* 1–11. https://doi.org/10.1186/s12951-019-0506-y

5 Bray, F., Ferlay, J., Soerjomataram, I., Siegel, R.L., Torre, L.A., & Jemal, A. (2018). Global cancer statistics 2018: GLOBOCAN estimates of incidence and mortality worldwide for 36 cancers in 185 countries. *CA. Cancer J. Clin., 68,* 394–424. https://doi.org/10.3322/caac.21492

6 Tietze, R., Zaloga, J., Unterweger, H., Lyer, S., Friedrich, R.P., & Janko, C. (2016). Magnetic nanoparticle-based drug delivery for cancer therapy. *Biochem. Biophys. Res. Commun., 468,* 463–470. https://doi.org/10.1016/J.BBRC.2015.08.022

7 Wolfram, J., & Ferrari M. (2019). Clinical cancer nanomedicine. *Nano Today., 25,* 85–98. https://doi.org/10.1016/j.nantod.2019.02.005

8 Remya, N.S., Syama, S., Sabareeswaran, A., & Mohanan, P.V. (2016). Toxicity, toxicokinetics and biodistribution of dextran stabilized Iron oxide Nanoparticles for biomedical applications. *Int. J. Pharm., 511,* 586–598. https://doi.org/10.1016/J.IJPHARM.2016.06.119

9 Chandra Mohanta, S., Saha, A., & Sujatha Devi P. (2018). PEGylated Iron Oxide Nanoparticles for pH Responsive Drug Delivery Application. *Mater. Today Proc., 5,* 9715–9125.

10 Hauser, A.K., Mitov, M.I., Daley, E.F., McGarry, R.C., Anderson K.W., & Hilt, J.Z. (2016). Targeted iron oxide nanoparticles for the enhancement of radiation therapy. *Biomaterials, 105,* 127–135. https://doi.org/10.1016/J.BIOMATERIALS.2016.07.032

11 Shelat, R., Chandra, S., & Khanna, A. (2018). Detailed toxicity evaluation of β-cyclodextrin coated iron oxide nanoparticles for biomedical applications. *Int. J. Biol. Macromol., 110,* 357–365. https://doi.org/10.1016/J.IJBIOMAC.2017.09.067

12 Dadfar, S.M., Roemhild, K., Drude, N.I., von Stillfried, S., Knüchel, R., & Kiessling F., et al. (2019). Iron oxide nanoparticles: Diagnostic, therapeutic and theranostic applications. *Adv. Drug Deliv. Rev., 138,* 302–325. https://doi.org/10.1016/J.ADDR.2019.01.005

13 Rajabi, F., Arancon, R.A.D., & Luque, R. (2015). Oxidative esterification of alcohols and aldehydes using supported iron oxide nanoparticle catalysts. *Catal. Commun., 59.,* 101–103. https://doi.org/10.1016/J.CATCOM.2014.09.022

14 Pizzolato, E., Scaramuzza, S., Carraro, F., Sartori, A., Agnoli, S., & Amendola, V. et al. (2016). Water oxidation electrocatalysis with iron oxide nanoparticles prepared via laser ablation. *J. Energy Chem., 25,* 246–250. https://doi.org/10.1016/J.JECHEM.2015.12.004

15 Devi, H.S., & Singh, T.D. (2016). Iron oxide nanoparticles synthesis through a benign approach and its catalytic application. *Perspect. Sci., 8,* 287–289.

16 Nebu, J., Anjali Devi, J.S., Aparna, R.S., Aswathy, B., Lekha, G.M., & Sony, G. (2018). Fluorescence turn-on detection of fenitrothion using gold nanoparticle quenched fluorescein and its separation using superparamagnetic iron oxide nanoparticle. *Actuators B Chem., 277,* 271–280. https://doi.org/10.1016/J.SNB.2018.08.153

17 van de Loosdrecht, M.M., Waanders, S., Krooshoop, H.J.G., & ten Haken, B. (2019). Separation of excitation and detection coils for in vivo detection of superparamagnetic iron oxide nanoparticles. *J. Magn. Magn. Mater., 475,* 563–569. https://doi.org/10.1016/J.JMMM.2018.12.012

18 Ozel, F., Tokay, E., Köçkar, F., & Köçkar, H. (2018). Characterization of tartaric acid and ascorbic acid coated iron oxide nanoparticles and their biocompatibility studies. *J. Magn. Magn. Mater., 474,* 654–660. https://doi.org/10.1016/J.JMMM.2018.12.012

19 Yathindranath, V., Sun, Z., Worden, M., Donald, L.J., & Thliveris, J.A. (2013). One-Pot Synthesis of Iron Oxide Nanoparticles with Functional Silane Shells: A Versatile General Precursor for Conjugations and Biomedical Applications. *Langmuir, 29,* 10850–10858.

20 Özgür, M., Ulu, A., Balcıoğlu, S., Özcan, İ., Köytepe, S., & Ateş, B. (2018). The Toxicity Assessment of Iron Oxide (Fe_3O_4) Nanoparticles on Physical and Biochemical Quality of Rainbow Trout Spermatozoon. *Toxics, 6,* 62. https://doi.org/10.3390/toxics6040062

21 Fernández-Bertólez, N., Costa, C., Brandão, F., Kiliç, G., Duarte, J.A., &Teixeira, J.P. et al. (2018). Toxicological assessment of silica-coated iron oxide nanoparticles in human astrocytes. *Food Chem. Toxicol., 118,* 13–23. https://doi.org/10.1016/J.FCT.2018.04.058

22 Janko, C., Zaloga, J., Pöttler, M., Dürr, S., Eberbeck, D., & Tietze, R. et al. (2017). Strategies to optimize the biocompatibility of iron oxide nanoparticles — «SPIONs safe by design. *J. Magn. Magn. Mater., 431,* 281–284. https://doi.org/10.1016/J.JMMM.2016.09.034

23 Kurczewska, J., Cegłowski, M., & Schroeder, G. (2018). Preparation of multifunctional cascade iron oxide nanoparticles for drug delivery. *Mater. Chem. Phys., 211,* 34–41. https://doi.org/10.1016/J.MATCHEMPHYS.2018.01.064

24 Tishkevich, D.I., Korolkov, I. V., Kozlovskiy, A.L., Anisovich, M., Vinnik, D.A., & Ermekova, A.E. et al. (2019). Immobilization of boron-rich compound on Fe_3O_4 nanoparticles: Stability and cytotoxicity. *J. Alloys Compd., 794,* 573–581. https://doi.org/10.1016/j.jallcom.2019.05.075

25 Kozlovskiy, A.L., Ermekova, A.E., Korolkov, I.V., Chudoba, D., Jazdzewska, M., & Ludzik, K. et al. (2019). Study of phase transformations, structural, corrosion properties and cytotoxicity of magnetite-based nanoparticles. *Vacuum, 163,* 236–247. https://doi.org/10.1016/J.VACUUM.2019.02.029

26 Stockert, J.C., Horobin, R.W., Colombo, L.L., & Blázquez-Castro, A. (2018). Tetrazolium salts and formazan products in Cell Biology: Viability assessment, fluorescence imaging, and labeling perspectives. *Acta Histochem., 120,* 159–167. https://doi.org/10.1016/j.acthis.2018.02.005

27 Abe, K., & Matsuki, N. (2000). Measurement of cellular 3-(4,5-dimethylthiazol-2-yl)-2,5-diphenyltetrazolium bromide (MTT) reduction activity and lactate dehydrogenase release using MTT. *Neurosci. Res., 38,* 325–329. https://doi.org/10.1016/S0168-0102(00)00188-7

28 Rubio, F., Rubio, J., & Oteo, J.L. (1998). A FT-IR study of the hydrolysis of Tetraethylorthoselicate (TEOS). *Spectrosc. Lett., 31,* 199–219. https://doi.org/10.1080/00387019808006772

29 Leites, L.A. (1992). Vibrational Spectroscopy of Carboranes and Parent Boranes and Its Capabilities in Carborane Chemistry. *Chem. Rev., 92,* 279–323.

30 Bondarenko, L.S., Kovel, E.S., Kydralieva, K.A., Dzhardimalieva, G.I., Illés, E., & Tombácz E. et al. (2020). Effects of Modified Magnetite Nanoparticles on Bacterial Cells and Enzyme Reactions. *Polymers, 10,* 1499. https://doi.org/10.3390/nano10081499

31 Bondarenko, L.S., Kahru, A., Terekhova, V., Dzhardimalieva, G., Uchanov, P., & Kydralieva, K. (2020). Effects of Humic Acids on the Ecotoxicity of Fe_3O_4 Nanoparticles and Fe-Ions: Impact of Oxidation and Aging. *Nanomaterials, 10,* 1–18. https://doi.org/10.3390/nano10102011

Information about authors

Korolkov, Ilya Vladimirovich (*corresponding author*) — PhD, senior researcher of the Institute of Nuclear Physics, Abylay khana 2/1, 010000, Nur-Sultan, Kazakhstan; e-mail: i.korolkov@inp.kz, https://orcid.org/0000-0002-0766-2803

Katarzyna, Ludzik — researcher of the University of Lodz, ul. Uniwersytecka 3, 90–137 Łódź, Poland; e-mail: katarzynaludzik82@gmail.com, https://orcid.org/0000-0003-1749-808X

Lisovskaya, Lana Igorevna — engineer of the Institute of Nuclear Physics, Abylay khana 2/1, 010000, Nur-Sultan, Kazakhstan; e-mail: ms.defrance@mail.ru.

Zibert, Aleksandr Vitalevich — student of L.N. Gumilyov Eurasian National University, Satbayev str., 2, 010000, Nur-Sultan, Kazakhstan; e-mail: alexandr.zibert@bk.ru.

Yeszhanov, Arman Bachitzhanovich — junior researcher of the Institute of Nuclear Physics, Abylay khana 2/1, 010000, Nur-Sultan, Kazakhstan; e-mail: arman_e7@mail.ru, https://orcid.org/0000-0002-1328-8678

Zdorovets, Maxim Vladimirovich — Director of the Institute of Nuclear Physics, Abylay khana 2/1, 010000, Nur-Sultan, Kazakhstan; e-mail: mzdorovets@inp.kz, https://orcid.org/0000-0003-2992-1375